

# The Scaling of the Redshift Power Spectrum: Observations from the Las Campanas Redshift Survey

Y.P. Jing<sup>1,2,3,4</sup>, G. Börner<sup>1,4,5</sup>

<sup>1</sup> Shanghai Astronomical Observatory, the Partner Group of MPI für Astrophysik, Nandan  
Road 80, Shanghai 200030, China

<sup>2</sup> National Astronomical Observatories, Chinese Academy of Sciences, Beijing 100012,  
China

<sup>3</sup> National Astronomical Observatory, Mitaka, Tokyo 181-8588, Japan

<sup>4</sup> Research Center for the Early Universe, School of Science, University of Tokyo,  
Bunkyo-ku, Tokyo 113, Japan

<sup>5</sup> Max-Planck-Institut für Astrophysik, Karl-Schwarzschild-Strasse 1, 85748 Garching,  
Germany

e-mail: ypjing@center.shao.ac.cn, grb@mpa-garching.mpg.de

Received —————; accepted —————

## ABSTRACT

In a recent paper we have studied the redshift power spectrum  $P^S(k, \mu)$  in three CDM models with the help of high resolution simulations. Here we apply the method to the largest available redshift survey, the Las Campanas Redshift Survey (LCRS). The basic model is to express  $P^S(k, \mu)$  as a product of three factors

$$P^S(k, \mu) = P^R(k)(1 + \beta\mu^2)^2 D(k, \mu). \quad (1)$$

Here  $\mu$  is the cosine of the angle between the wave vector and the line of sight. The damping function  $D$  for the range of scales accessible to an accurate analysis of the LCRS is well approximated by the Lorentz factor

$$D = [1 + \frac{1}{2}(k\mu\sigma_{12})^2]^{-1}. \quad (2)$$

We have investigated different values for  $\beta$  ( $\beta = 0.4, 0.5, 0.6$ ), and measured the real space power spectrum  $P^R(k)$  and the pairwise velocity dispersion  $\sigma_{12}(k)$  from  $P^S(k, \mu)$  for different values of  $\mu$ . The velocity dispersion  $\sigma_{12}(k)$  is nearly a constant from  $k = 0.5$  to  $3 \ h\text{Mpc}^{-1}$ . The average value for this range is  $510 \pm 70 \text{ km s}^{-1}$ . The power spectrum  $P^R(k)$  decreases with  $k$  approximately with  $k^{-1.7}$  for  $k$  between  $0.1$  and  $4 \ h\text{Mpc}^{-1}$ . The statistical significance of the results, and the error bars, are found with the help of mock samples constructed from a large set of high resolution simulations. A flat, low-density ( $\Omega_0 = 0.2$ ) CDM model can give a good fit to the data, if a scale-dependent special bias scheme is used which we have called the cluster-under-weighted bias (Jing et al.).

*Subject headings:* galaxies: clustering - galaxies: distances and redshifts - large-scale structure of Universe - cosmology: theory - dark matter

## 1. Introduction

The spatial distribution of galaxies can be retrieved approximately, when the redshift is used as a measure of the distance. It is not exact, because the galaxies in general deviate from the linear Hubble flow, but the redshift distortions can provide us with valuable information about the dynamics of galaxies. A traditional method for studying the redshift distortion is the redshift two-point correlation function (RTPCF)  $\xi_z(r_p, \pi)$  (Geller & Peebles 1973, Peebles 1980, Bean et al. 1983, Davis & Peebles 1983 Mo, Jing & Börner 1993, Marzke et al. 1995, Fisher, et al. 1994, Ratcliffe et al. 1998, Postman et al. 1998, Grogin & Geller 1999, Small et al. 1999). Assuming certain functional forms for the distribution function (DF) of the pairwise velocity (say, an exponential form, Peebles 1976) and for the average infall velocity (say, the form of the self-similar solution, Davis & Peebles 1983), one can construct a model for  $\xi_z(r_p, \pi)$  which describes the real situation, when the coupling between the peculiar velocity and the spatial density of the galaxies is weak (Peebles 1980). A comparison of the model with observations for  $\xi_z(r_p, \pi)$  provides a test for the validity of the model assumptions (such as the DF of the pairwise velocity) and a determination of the pairwise velocity dispersion  $\sigma_{12}(r)$ . Early studies of small redshift samples (Peebles 1976, Peebles 1979) have shown that an exponential form for the DF of the pairwise velocity is preferable to a Gaussian form. This important conclusion has been confirmed by a number of later studies based on much larger surveys ( Davis & Peebles 1983, Marzke et al. 1995, Fisher, et al. 1994). The pairwise velocity dispersion was not easy to pin down; the value sensitively depends on the presence or absence of rare rich clusters in the redshift surveys which contained only a few thousand galaxies (Mo, Jing & Börner 1993, Zurek et al 1994, Marzke et al. 1995). Motivated by this fact, several authors have since attempted (Kepner, Summers & Strauss 1997, Davis, Miller & White 1997, Strauss, Ostriker & Cen 1998, Baker, Davis & Lin 2000) to find new statistics for the thermal motion of galaxies which are less sensitive to the regions of rich clusters. The new statistics, by their design,

are more robust with respect to the sampling of rich clusters than the pair-weighted  $\sigma_{12}(r)$  and have produced interesting constraints on models of galaxy formation, but the results sometimes are more difficult to interpret in the context of dynamical theories (e.g. the Cosmic Virial Theorem and the Cosmic Energy Equation). Fortunately, the pair-weighting will no longer be a problem for future large redshift surveys like 2dF and SDSS which will contain hundreds to thousands of rich clusters in the survey. In fact, the currently largest publicly available redshift survey, the Las Campanas Redshift Survey (LCRS; Shectman et al. 1996) which contains about 30 rich clusters, is already large enough to reduce the sampling error in  $\sigma_{12}(r)$  to 15% only (Jing, Mo & Börner 1998, hereafter JMB98). Therefore the pairwise velocity dispersion, which is a well-defined physical quantity and has simple relations to the dynamical theories (the Virial Theorem), will remain an important quantity to measure in observations.

Although the pair-weighting is not a problem for the statistics of  $\sigma_{12}(r)$  with the largest redshift surveys or the next generation of redshift surveys, the currently widely used method of measuring  $\sigma_{12}(r)$  (Davis & Peebles 1983) does have its limitations (JMB98). Functional forms must be first assumed for the DF of the pairwise velocity and the infall velocity, and it must be assumed that the spatial density and peculiar velocity of galaxies are uncorrelated so that the redshift two-point correlation function (model) can be written as a convolution of the real-space correlation with the DF of the pairwise velocity. Although the validity of the functional form for the DF of the pairwise velocity can be checked by comparing the model of the RTPCF to the observed one, the tests of different functional forms are rather limited. The functional form may depend on the separation between the objects (Juszkiewicz, Fisher & Szapudi 1998, Magira, Jing & Suto 2000). The infall velocity also has a significant effect on the determination of  $\sigma_{12}(r)$ , because the two quantities are rather degenerate in modeling  $\xi_z(r_p, \pi)$  (Jing & Börner 1998). Moreover, the density and velocity are strongly coupled at the small scales where previous studies have measured  $\sigma_{12}(r)$ . These

limitations can lead to some systematic bias in the estimation of  $\sigma_{12}(r)$  (JMB98; Jing & Börner 1998). These systematic effects were not so important in early statistical studies of  $\sigma_{12}(r)$  since the sampling errors in  $\sigma_{12}(r)$  were dominant. Since the sampling error is just 15% for the LCRS (JMB98) and will be even smaller for the upcoming surveys, it is important to consider alternative methods to measure the redshift distortion and  $\sigma_{12}(r)$  which are less model dependent.

In a recent paper (Jing & Börner 2001, hereafter JB2001), we have studied the redshift power spectrum  $P^S(k, \mu)$  in three typical CDM cosmological models, where  $\mu$  is the cosine of the angle between the wave vector and the line-of-sight. Two distinctive biased tracers, the primordial density peaks (Bardeen et al. 1986; Davis et al. 1985) and the cluster-under-weighted population of particles (JMB98), are considered in addition to the pure dark matter models. Based on a large set of high-resolution simulations, we have measured the redshift power spectrum for these three tracers from the linear to the non-linear regimes. For all the tracers and the three CDM models, the redshift power spectrum  $P^S(k, \mu)$  can be expressed by

$$P^S(k, \mu) = P^R(k)(1 + \beta\mu^2)^2 D(k\mu\sigma_{12}(k)) \quad (3)$$

where  $P^R(k)$  is the real space power spectrum, and  $\beta = \Omega^{0.6}/b$  ( $\Omega$  is the density parameter and  $b$  is the linear bias parameter). The factor  $(1 + \beta\mu^2)^2$  accounts for the linear compression of structures on large scales (Kaiser 1987). Although  $\sigma_{12}(k)$  and the 3-D peculiar velocity dispersion are not immediately comparable, it was pointed out in JB2001 that their values are different only by 15% in the simulation, if  $r = 1/k$  is used in the comparison. So  $\sigma_{12}(k)$  is a good indicator for the velocity dispersion. In Equation (3) the damping function  $D$ , which should generally depend on  $k$ ,  $\mu$  and  $\sigma_{12}(k)$ , is a function of one variable  $k\mu\sigma_{12}(k)$  only. The functional form of  $D(k\mu\sigma_{12}(k))$  was found to depend on the cosmological model and the bias recipes, but for small  $k$  (large scales) where  $D > 0.1$ ,  $D(k\mu\sigma_{12}(k))$  can be

accurately expressed by the Lorentz form,

$$D(k\mu\sigma_{12}(k)) = \frac{1}{1 + \frac{1}{2}k^2\mu^2\sigma_{12}^2(k)}. \quad (4)$$

This implies that the exponential form is a good model for the distribution function of the pairwise velocity at large separation. Applying the model of Equation (3) to an observation of  $P^S(k, \mu)$  therefore may yield a determination for the four quantities:  $P^R(k)$ ,  $\beta$ ,  $\sigma_{12}(k)$  and the functional form of  $D(y)$  all of which are useful observables for testing galaxy formation models. An additional advantage is that the infall effect is accounted for by the single parameter  $\beta$ , compared with a complicated form for the infall velocity used in the correlation function method.

In this paper, we apply this method to the LCRS, the largest redshift survey publicly available. The redshift power spectrum  $P^S(k, \mu)$  is measured from the RTPCF  $\xi_z(r_p, \pi)$  of this survey (JMB98) using the method outlined in Section 2. The result is presented in section 3. The statistical significance of the measurement, and the error bars, is tested using mock samples in section 4. The final section (§5) is devoted to discussion and conclusions.

## 2. Method

We convert the redshift two-point correlation function  $\xi_z(\mathbf{s})$  to the redshift power spectrum by the Fourier transformation:

$$P^S(\mathbf{k}) = \int \xi_z(\mathbf{s}) e^{-i\mathbf{k}\cdot\mathbf{s}} d\mathbf{s}. \quad (5)$$

In cylindrical polar coordinates  $(r_p, \phi, \pi)$  with the  $\pi$ -axis parallel to the line-of-sight,  $P^S(\mathbf{k})$  depends on  $k_p$ , the wavenumber perpendicular to the line-of-sight, and on  $k_\pi$ , the wavenumber parallel to the line-of-sight. The power spectrum can be written

$$P^S(k_p, k_\pi) = \int \xi_z(r_p, \pi) e^{-i[k_p r_p \cos(\phi) + \pi k_\pi]} r_p dr_p d\phi d\pi. \quad (6)$$

With some elementary mathematical manipulation, we get the following expression:

$$P^S(k_p, k_\pi) = 2\pi \int_{-\infty}^{\infty} d\pi \int_0^{\infty} r_p dr_p \xi_z(r_p, \pi) \cos(k_\pi \pi) J_0(k_p r_p) \quad (7)$$

where  $J_0(k_p r_p)$  is the zeroth-order Bessel function.

We will use the redshift two-point correlation function  $\xi_z(r_p, \pi)$  of the LCRS measured by JMB98. In their paper, JMB98 analyzed the correlation function for the whole sample as well as for the three southern slices and the three northern slices separately. Moreover, they have generated a large sample of mock surveys with different observational selection effects and measured  $\xi_z(r_p, \pi)$  for them. Their tests with the mock samples are very important, as emphasized by JMB98 themselves, for checking the statistical methods, correcting for the observational selection effects, and estimating the statistical errors of the measurements. We will also use their results of the mock samples in this paper for the same purposes.

In their work, JMB98 measured  $\xi_z(r_p, \pi)$  in equal logarithmic bins of  $r_p$  and in equal linear bins of  $\pi$ . The reason why different types of bins are chosen for  $r_p$  and  $\pi$  is the fact that  $\xi_z(r_p, \pi)$  decreases rapidly with  $r_p$  but is flat with  $\pi$  on small scales. Thus this way of presenting  $\xi_z(r_p, \pi)$  is better than using the log-log or the linear-linear bins for  $r_p$  and  $\pi$ , and is also suitable for the present work. The peculiar velocity of a few hundred  $\text{km s}^{-1}$  should smoothen out structures on a few  $h^{-1}\text{Mpc}$  in the radial direction, and the linear bin of  $\Delta\pi_i = 1 h^{-1}\text{Mpc}$  is suitable for resolving the structures in the radial direction. With logarithmic bins chosen for  $r_p$ , the  $r_p$  dependence is resolved well, because otherwise the small scale clustering on the projected direction cannot be recovered. With this bin method, we obtain the power spectrum:

$$P^S(k_p, k_\pi) = 2\pi \sum_{i,j} \Delta\pi_i r_{p,j}^2 \Delta \ln r_{p,j} \xi_z(r_{p,j}, \pi_i) \cos(k_\pi \pi_i) J_0(k_p r_{p,j}) \quad (8)$$

where  $\pi_i$  runs from  $-50$  to  $50 h^{-1}\text{Mpc}$  with  $\Delta\pi_i = 1 h^{-1}\text{Mpc}$  and  $r_{p,j}$  from  $0.1$  to  $31.6 h^{-1}\text{Mpc}$  with  $\Delta \ln r_{p,j} = 0.288$  (Be careful not to confuse two  $\pi$ s in Eqs. (7) and (8):

the first  $\pi$  in the right-hand-side has the conventional meaning, i.e. 3.14159..., and the others are for the axis along the line-of-sight.). We use the summation of Eq.(8) with rectangular boundaries in  $\pi$  and  $r_p$ . This gives good, unbiased results for both the velocity dispersion and the power spectrum, as will be seen in §4. This works also better than a spherical window of radially decreasing weighting which tends to bias the power spectrum estimates. We have tested this thoroughly comparing the results for mock samples with those for the full simulation.

There are several sources which could introduce errors to our measurement of the redshift power spectrum. One is the Poisson error related to the discrete sampling of galaxies, and the other is the cosmic variance related to the limited volume of the survey. Both types of uncertainty are intrinsic for any redshift survey, and are already factored into the measured  $\xi_z(r_p, \pi)$ . When converting the correlation function to the power spectrum with Eq.(8), the finite bins and the cutoffs of  $r_p$  and  $\pi$  may cause additional errors. To reduce the effect of the finite bins, we divide every  $\pi$  and  $\ln r_p$  bin into  $N$  sub-bins, and use the cubic spline method to interpolate  $\xi_z(r_p, \pi)$ . We have run a number of trials for different numbers of the sub-bins  $N$ , and found that the final result is insensitive to  $N$ . For the results presented in the following sections,  $N = 10$  is used. Since these different types of errors are mixed in a complicated way in the measured power spectrum, we will use the mock samples to quantify the errors.

Landy, Szalay & Broadhurst (1998) have also considered the Fourier transform of the redshift two-point correlation function for the LCRS survey. Although the spirit of their work and ours is similar, there are some important differences. We have included the infall effect in our statistics and consider the full angular  $\mu$ -dependence of the redshift power spectrum. Furthermore, we will use the two dimensional integral (Eq.7) to determine both the velocity dispersion and the power spectrum.



### 3. The redshift power spectrum in the Las Campanas redshift survey

Since the redshift distortion does not change the total number of the galaxy pairs at a certain projected distance, it is not difficult to prove from Eq.(3) that  $P^S(k, 0) = P^R(k)$ . Thus the damping factor  $D(k, \mu)$  can be estimated by the following expression

$$D(k, \mu) \equiv \frac{P^S(k, \mu)}{P^S(k, 0)(1 + \beta\mu^2)^2}. \quad (9)$$

The quantities on the right hand side can be measured through Eq.(8) except for the parameter  $\beta$ . If the observational catalog is large enough, one can simultaneously determine the damping factor and  $\beta$  as described by JB2001. However, the LCRS is too small to measure this quantity because, as we can see in Figure 1, there is a large statistical fluctuation on large scales ( $k\sigma_v\mu \lesssim 1$ ). This is consistent with the recent estimates of Matsubara et al. (2000) based on an eigenmode method, who give  $\beta = 0.30 \pm 0.39$ . Therefore, we will not attempt to determine the value of  $\beta$ . Instead we will focus on measuring the damping function. Here we fix a value for  $\beta$ ,  $\beta = 0.5$ , which is consistent with the observations of the cluster abundance (e.g. Kitayama & Suto 1996) as well as with the statistical result of Matsubara et al (2000) for the LCRS. We have checked the results for  $\beta = 0.4$  and  $\beta = 0.6$ , and found that our conclusions are little changed if  $\beta$  varies within this range.

Figure 1 shows the inverse of the damping function  $D(k, \mu)$  we measured for the Las Campanas redshift survey. Following JB2001, the damping factor is expressed as a function of the scaling variable  $k\mu\sigma_v$ . For this figure,  $\sigma_v$  is fixed to be a constant  $500 \text{ km s}^{-1}$ , and only the data points which have a relative error smaller than 50% are presented. The error of  $D(k, \mu)$  is estimated from the scatter of this quantity between the cluster-weighted mock samples (see §4 about the mock samples). From the figure, it is easy to see that our measured result of  $D(k, \mu)$  can be well described by a Lorentz form (the solid line). This result is consistent with the model studies of JB2001 who have shown that the damping

factors of different bias models are all very close to the Lorentz form when the damping factor  $D(k, \mu) \gtrsim 0.1$ . The LCRS is still not large enough to explore the highly non-linear regime where  $D(k, \mu) \ll 0.1$ . This also means that an exponential distribution function for the pairwise velocities is a good approximation in this range. In addition, we note that there exists significant scatter on large scales  $k\mu\sigma_v < 1$ , thus it is very difficult to measure the  $\beta$  value accurately with this catalog (cf. Matsubara et al. 2000).

As Figure 1 shows, the damping function that the LCRS can explore is in the interval  $0.1 \lesssim D(k, \mu) < 1$ . The accuracy is limited by the sample-to-sample error (the cosmic variance) on large scale ( $D(k, \mu) \approx 1$ ). Since the LCRS measured the redshift for each  $1.5 \times 1.5 \text{ deg}^2$  field by one exposure, the dense regions in the galaxy distribution (e.g. clusters) are under sampled, which seriously limits the accuracy of our measurement for small scales [ $D(k, \mu) \ll 1$ ]. For the regime which the LCRS can effectively explore, the Lorentz form is a good approximation for the damping function, consistent with the model study of JB2001. Thus, we can determine the real-space power spectrum  $P^R(k)$  and the pairwise velocity dispersion  $\sigma_v$  by a least-square fitting to the observed redshift power spectrum, assuming the Lorentz form for the damping factor. Although  $P^R(k) \equiv P^S(k, 0)$  mathematically, for a finite-sized survey like the LCRS,  $P^S(k, 0)$  fluctuates around the true value of  $P^R(k)$  for the limited number of the modes. We can better determine  $P^R(k)$  if we combine  $P^S(k, \mu)$  at different angles  $\mu$ , thus we treat  $P^R(k)$  as a free parameter.

We show such best fitting curves (the solid lines) together with the measured redshift power spectrum in Figure 2. For the curves from top to bottom, the wavenumber  $k$  is incremented by  $\Delta \lg k = 0.2$  from  $0.25 \text{ hMpc}^{-1}$  to  $2.5 \text{ hMpc}^{-1}$ . As the figure shows, the model we use for  $P^S(k, \mu)$  (i.e. the Lorentz form for the damping function and equation 3) succeeds in describing the result of the LCRS data. Our best fitting values for  $\sigma_{12}(k)$  and  $P^R(k)$  are plotted in Figures 3 and 4 respectively. Here we have corrected the *fiber collision*

*effect of the survey* (Shectman et al. 1996) for both quantities following the procedure of JMB98. The error bars shown in these figures are simply the standard deviations for identical analyses of the 60 mock samples. We have also used the bootstrap method to estimate the errors, and found that the bootstrap errors are typically 30 ~ 50% smaller than the errors determined from the mock samples. We prefer to adopt the mock errors, because they have adequately included the sample-to-sample variations (i.e. cosmic variances).

In addition, the mock errors are not sensitive to the bias model used; the mock samples constructed from the dark matter particles give similar error estimates (cf. JMB98). The velocity dispersion  $\sigma_{12}(k)$  is nearly a constant from 0.5 to  $3 h\text{Mpc}^{-1}$ . The average of  $\sigma_{12}(k)$  for this  $k$  range is  $510 \pm 70 \text{ km s}^{-1}$ . This error bar for the averaged  $\sigma_{12}(k)$  is only slightly smaller than the typical error  $\sim 90 \text{ km s}^{-1}$  of each individual  $k$  bin, since the errors of individual  $k$  bins are correlated. Our result for  $\sigma_{12}(k)$  is in good agreement with our previous determination  $570 \pm 80 \text{ km s}^{-1}$  at a separation of  $r = 1 h^{-1}\text{Mpc}$  based on a fit to the two-point correlation function (JBM98). A reasonable change for the  $\beta$  value from 0.4 to 0.6 based on the cluster abundance observations (e.g. Kitayama & Suto 1996) leads to a change of 5 ~ 10% in  $\sigma_{12}(k)$ . The south (dashed lines) and north (dotted lines) subsamples give a result consistent with the whole sample within the statistical uncertainty.

Our measurement for the power spectrum  $P^R(k)$  is presented in Figure 4. The spectrum is approximately a power law for the range of scales that the LCRS can explore. It decreases with  $k$  approximately as  $\propto k^{-1.7}$  for  $0.1 \lesssim k \lesssim 4 h\text{Mpc}^{-1}$ . We consider this result very reliable, because we have tested our method of a direct Fourier transform extensively with mock samples. In our tests we found that this method is superior to using other types of window functions, e.g. spherical ones, especially when the aim is to obtain unbiased estimates of  $\sigma_{12}$  and  $P(k)$ . These results are qualitatively in agreement with the real space power spectrum of the APM survey (Baugh & Efstathiou, 1994). The shoulder at  $k \approx 0.4 h\text{Mpc}^{-1}$  apparent in Figure 4 appeared also in the APM results (their Figure 11)

at exactly the same scale, though the error bars of the LCRS are much larger. We also note that the power-law index of  $P(k)$  for  $0.4 \lesssim k \lesssim 4 h\text{Mpc}^{-1}$  is  $\approx -1.2$  compared with  $\approx -1.3$  of the APM survey.

#### 4. Mock samples and test of the method

As we discussed in Section 2, there are several possible sources which could introduce errors to our measured redshift power spectrum and to our fitted quantities. The use of the finite bins and the cutoffs in the radial and projected separations may lead to a certain systematic bias in the measured power spectrum. When we write down equation (3), we implicitly make the distant observer assumption. There are also statistical uncertainties in the power spectrum which are related to the cosmic variance and the Poisson error inherent to a redshift survey. All these uncertainties, systematic or statistical, are however difficult to model with an analytical method. Fortunately, they can be easily quantified with the help of the mock samples.

We will use the mock samples of JMB98 which were produced from a set of CDM N-body simulations of 2 million particles. Three flat CDM models were considered: one is the once standard CDM model of the density parameter  $\Omega_0 = 1$  and the normalization  $\sigma_8 = 0.62$ , and the other two are low-density flat CDM universes with parameters  $(\Omega_0, \sigma_8) = (0.2, 1)$  and  $(0.3, 1)$  respectively. The known selection effects of the survey, including the sky boundaries, the limiting magnitudes and the redshift selection function, the observed rate due to the limited number of fibers, and the missing galaxies due to the fiber mechanical collision, were properly simulated in the mock samples. Because the CDM models were found to have too steep a two-point correlation and too large a pairwise velocity dispersion compared to the LCRS result, JMB98 have introduced a simple bias model which under weights the cluster regions in the dark matter models. The mock samples based on this

bias model yielded much better matches to the LCRS observation, and the model of  $(\Omega_0, \sigma_8) = (0.2, 1)$  was shown to be consistent with the observations.

To test our statistical method, we will use two types of mock samples of the cluster weighted  $\Omega = 0.2$  sample. To test if there is any systematic bias with the method, we will use mock samples which incorporate all selection effects except the fiber collision. The reason why we exclude the fiber collision effect is because it is not possible to include this effect in a 3-D simulation sample, as the results of the 3-D sample must be compared with those of the mock samples in the test. To quantify the statistical errors of our measured quantities, we will use the mock samples based on the cluster-weighted  $\Omega_0 = 0.2$  sample with the fiber collision effect. For these mock samples, we will include or exclude the fiber collision effect in order to measure the systematic effect of the fiber collision.

Figure 5 presents our determination of the damping function in the cluster-weighted mock samples of  $\Omega_0 = 0.2$  according to Equation (9). The right panel shows the result for one mock sample which is randomly chosen. The damping function can be approximated by a Lorentz function (the solid line) within the scatter as in the LCRS observation. If we increase the number of mock samples to 60 and thus reduce the noise, the mean damping function decreases slightly faster than the Lorentz form at  $k\mu\sigma_v \gtrsim 3$  (left panel). This behavior was also found by JB2001 for the same model who measured the damping function by FFT for the full simulations (thus achieving higher accuracy). In fact, the mean damping function is not only qualitatively but also quantitatively in good agreement with the results of JB2001. This test indicates that our determinations for the damping function are not systematically biased, though there still exist considerable scatter for the LCRS. With the upcoming large surveys 2dF and SDSS, we expect that the uncertainties of the redshift power spectrum will be considerably reduced and it will become practical to measure a damping function which can be used to discriminate between theoretical models.

For the LCRS, however, the Lorentz form is still sufficiently accurate for a description of the damping function.

Using the Lorentz form for the damping function, we determine the pairwise velocity dispersion  $\sigma_{12}(k)$  and the real-space power spectrum  $P^R(k)$  for the mock samples of the  $\Omega_0 = 0.2$  model in the same way as for the real catalog LCRS. These two quantities are measured for each of the 60 samples, and the mean values and the expected  $1\sigma$  errors of the mean values are plotted in Figure 6 (symbols with error bars). The agreement is quite satisfactory with the same two quantities measured from the true particle velocity and positions in the simulation (solid lines,  $k = 1/r$  for the pairwise velocity dispersion). The plots in Figure 6 demonstrate that this method to estimate  $\sigma_{12}(k)$  and  $P^R(k)$  works well, and does not suffer from a strong bias. There does exist some small systematic bias, as appeared in the estimated velocity dispersion  $\sigma_{12}(k)$  at  $k \approx 0.3 \text{ hMpc}^{-1}$  and  $k \approx 1.5 \text{ hMpc}^{-1}$ , which is likely caused by the sharp cutoffs in the radial and projected separations and can be removed by estimating RTPCF to larger separations.

Next we compare our statistical results with the predictions of the CDM models using the cluster-weighted bias. The results are shown in Figure 7. For the model with  $\Omega_0 = 1$ , we have shifted the power spectrum by the factor  $1/\sigma_8^2$ , assuming a linear bias of  $1/\sigma_8$ . The power spectra are consistent with the LCRS observation for the range of scales explored by the survey, but the velocity dispersions of the CDM models are still systematically higher than the observation. Only the CDM model with the density parameter  $\Omega_0 = 0.2$  is consistent with the observations. Its  $1\sigma$  lower limit actually coincides with the LCRS result. Just as in JMB98 we may conclude that the flat, low-density models give a better fit to the data than high-density CDM models. The cluster-weighted bias improves the agreement between models and data remarkably. From Fig.6 we can see that without the cluster-weighted bias (dotted lines) the velocity dispersion would increase by roughly

$100 \text{ km s}^{-1}$ , and the power spectrum in real space would be about 2 times higher. Similar changes could be seen in Fig.7, if the cluster-weighted bias were removed from the model calculations.

In a previous paper (JB2001) we have shown that the bias model using primordial density peaks gives even higher values for  $\sigma_{12}(k)$  and  $P^R(k)$ , since the clusters have more weight than the dark matter particles in that scheme. These arguments carry over to the analysis of the LCRS data. It seems that a preference for the cluster-weighted bias emerges from our analysis.

## 5. Discussions and conclusions

Here we want to comment briefly on some previous work on the determination of the pairwise velocity dispersion  $\sigma_{12}$  for the LCRS. In JMB98  $\sigma_{12}$  has been determined based on the traditional method of fitting the RTPCF. A value of  $\sigma_{12} = 570 \pm 80 \text{ km s}^{-1}$  at  $r_p = 1 h^{-1} \text{ Mpc}$  has been obtained, but figure 1 of JMB98 shows that this quantity is slightly smaller (about 450 to 500  $\text{km s}^{-1}$ ) at smaller ( $r_p \lesssim 0.3 h^{-1} \text{ Mpc}$ ) or larger ( $r_p \gtrsim 3 h^{-1} \text{ Mpc}$ ) separations. Since some difference between the quantities in Fourier space and coordinate spaces is expected, we regard our result in this paper,  $\sigma_{12} = 510 \pm 70 \text{ km s}^{-1}$  around  $k = 1 h \text{ Mpc}^{-1}$ , to be in excellent agreement with the result of JMB98 as well as the recent results of Ratcliffe et al. (1998). The value is larger than that Landy et al (1998) obtained based on a power spectrum analysis of the LCRS who ignored the infall effect and considered  $P^s(k, \mu)$  at  $\mu = (0, 1)$  only. In addition, the estimate of the power spectrum  $P^R(k)$  for the LCRS as a direct derivation from the redshift power spectrum seems a reliable result in the interval between  $0.1 h \text{ Mpc}^{-1}$  and  $3 h \text{ Mpc}^{-1}$ . We suspect that guesses at  $P^R(k)$  for larger scales (smaller  $k$ ) suffer from the sample variation of the LCRS.

We reach the following conclusions:

- The power spectrum  $P^R(k)$ , and the pairwise velocity dispersion  $\sigma_{12}(k)$  can be estimated reliably from the redshift power spectrum of the LCRS. An assumed form for the distribution function of the pairwise velocity is not needed, although it turns out that the damping function fits reasonably well to the Lorentz form, over an interval in  $k$  from  $0.1 h\text{Mpc}^{-1}$  to  $3 h\text{Mpc}^{-1}$ . The Lorentz form for the damping function is the Fourier transform of the exponential distribution of the pair velocities. The fact that over a range of the scales the Lorentz form is a satisfactory approximation shows that in a corresponding range of  $r$ -scales, the exponential distribution is a good model. A value for  $\beta$  must be assumed, but it has been reasonably determined by other observations.
- The last values are  $\sigma_{12}(k) = 510 \pm 70 \text{ km s}^{-1}$  from  $k = 0.5$  to  $3 h\text{Mpc}^{-1}$ , in agreement with JMB98;  $P^R(k) \propto k^{-1.7}$  for  $k = 0.1$  to  $4 h\text{Mpc}^{-1}$ .
- Very important is the extensive use of mock samples which are constructed from a large set of high resolution simulations. They allow us to estimate the errors and the statistical significance of the results reliably, despite the intricate way which various error producing effects interact.
- We find reasonable fits to these measured quantities only in flat, low-density CDM models with a cluster-weighted bias. This antibias model—the number of galaxies per unit mass in a massive cluster is proportional to  $M^\alpha$  ( $M$  is the cluster mass) – suggested in JMB98 obviously deserves attention in future work. It should be pointed out that the parameter  $\alpha = -0.08$  used in this paper corresponds to a particular selection of galaxies: the LCRS galaxies. For other mix of galaxies (i.e., other observational criteria),  $\alpha$  could be different. In our recent work (in preparation), we



found the bias model of  $\alpha = -0.25$  can successfully account for the clustering of IRAS galaxies.

- The method applied here would be more powerful in samples larger than the LCRS. The power spectrum  $P^R(k)$ , the  $\beta$ -value, pairwise velocity dispersion, and the damping function can all be determined simultaneously, if the data are good enough.

We are grateful to Yasushi Suto for the hospitality extended to us at the physics department of Tokyo university where most of the computation was completed. J.Y.P. gratefully acknowledges the receipt of a NAO COE foreign research fellowship. The work is supported in part by the One-Hundred-Talent Program, by NKBRSF(G19990754) and by NSFC to Y.P.J., and by SFB375 to G.B..

## REFERENCES

- Baker, J. E., Davis, M. & Lin, H. 2000, ApJ, 536, 112
- Bardeen, J. M., Bond, J. R., Kaiser, N. & Szalay, A. S. 1986, ApJ, 304, 15
- Bean A.J., Efstathiou G., Ellis R.S., Peterson B.A., Shanks T., 1983, MNRAS, 205, 605
- Baugh C.M., Efstathiou G., 1994, MNRAS, 267, 323
- Carlberg, R. G., Yee, H. K. C., Ellingson, E., Abraham, R., Gravel, P., Morris, S. & Pritchet, C. J. 1996, ApJ, 462, 32
- Davis M., Efstathiou G., Frenk C. S., White S. D. M., 1985, ApJ, 292, 371
- Davis, M., Miller, A. & White, S. D. M. 1997, ApJ, 490, 63
- Davis, M. & Peebles, P. J. E. 1983, ApJ, 267, 465
- Fisher, K. B., Davis, M., Strauss, M. A., Yahil, A. & Huchra, J. P. 1994, MNRAS, 267, 927
- Geller, M. J. & Peebles, P. J. E. 1973, ApJ, 184, 329
- Grogin, N. A. & Geller, M. J. 1999, AJ, 118, 2561
- Jing, Y. P. & Börner, G. 1998, ApJ, 503, 37
- Jing, Y. P. & Börner, G. 2001, ApJ, 547, 545
- Jing, Y. P., Mo, H. J. & Börner, G. 1998, ApJ, 494, 1
- Juszkiewicz, R., Fisher, K. B. & Szapudi, I. 1998, ApJ, 504, L1
- Kaiser, N. 1987, MNRAS, 227, 1
- Kepner, J. V., Summers, F. J. & Strauss, M. A. 1997, New Astronomy, 2, 165

- Kitayama, T. & Suto, Y. 1996, ApJ, 469, 480
- Landy, S. D., Szalay, A. S. & Broadhurst, T. J. 1998, ApJ, 494, L133
- Magira, H. , Jing, Y. P. & Suto, Y. 2000, ApJ, 528, 30
- Marzke, R. O., Geller, M. J., da Costa, L. N. & Huchra, J. P. 1995, AJ, 110, 477
- Matsubara, T., Szalay, A. S. & Landy, S. D. 2000, ApJ, 535, L1
- Mo, H. J., Jing, Y. P. & Börner, G. 1993, MNRAS, 264, 825
- Peebles, P. J. E. 1976, Ap&SS, 45, 3
- Peebles, P. J. E. 1979, AJ, 84, 730
- Peebles P.J.E., 1980, The Large-Scale Structure of the Universe, Princeton University Press,  
Princeton
- Postman, M., Lauer, T. R., Szapudi, I. . & Oegerle, W. 1998, ApJ, 506, 33
- Ratcliffe, A., Shanks, T., Parker, Q. A. & Fong, R. 1998, MNRAS, 296, 191
- Shectman S. A., Landy, S.D., Oemler A., Tucker D.L., Lin H., Kirshner R.P., Schechter P.L.,  
1996, ApJ, 470, 172
- Small, T. A., Ma, C. -P. , Sargent, W. L. W. & Hamilton, D. 1999, ApJ, 524, 31
- Strauss, M. A., Ostriker, J. P. & Cen, R. 1998, ApJ, 494, 20
- Zurek, W. H., Quinn, P. J., Salmon, J. K. & Warren, M. S. 1994, ApJ, 431, 559

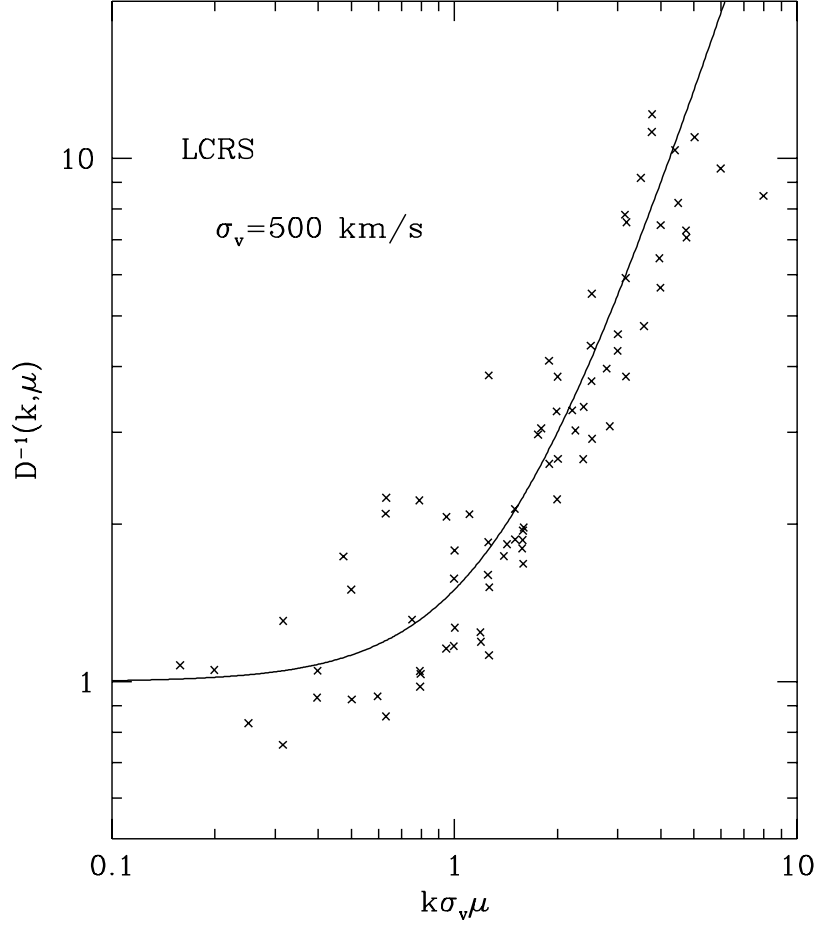


Fig. 1.— The inverse of the damping function  $D(k, \mu)$  of the Las Campanas Redshift Survey, plotted as a function of  $k\mu\sigma_v$ . In this plot, we have taken  $\beta = 0.5$  and  $\sigma_v = 500 \text{ km s}^{-1}$ .

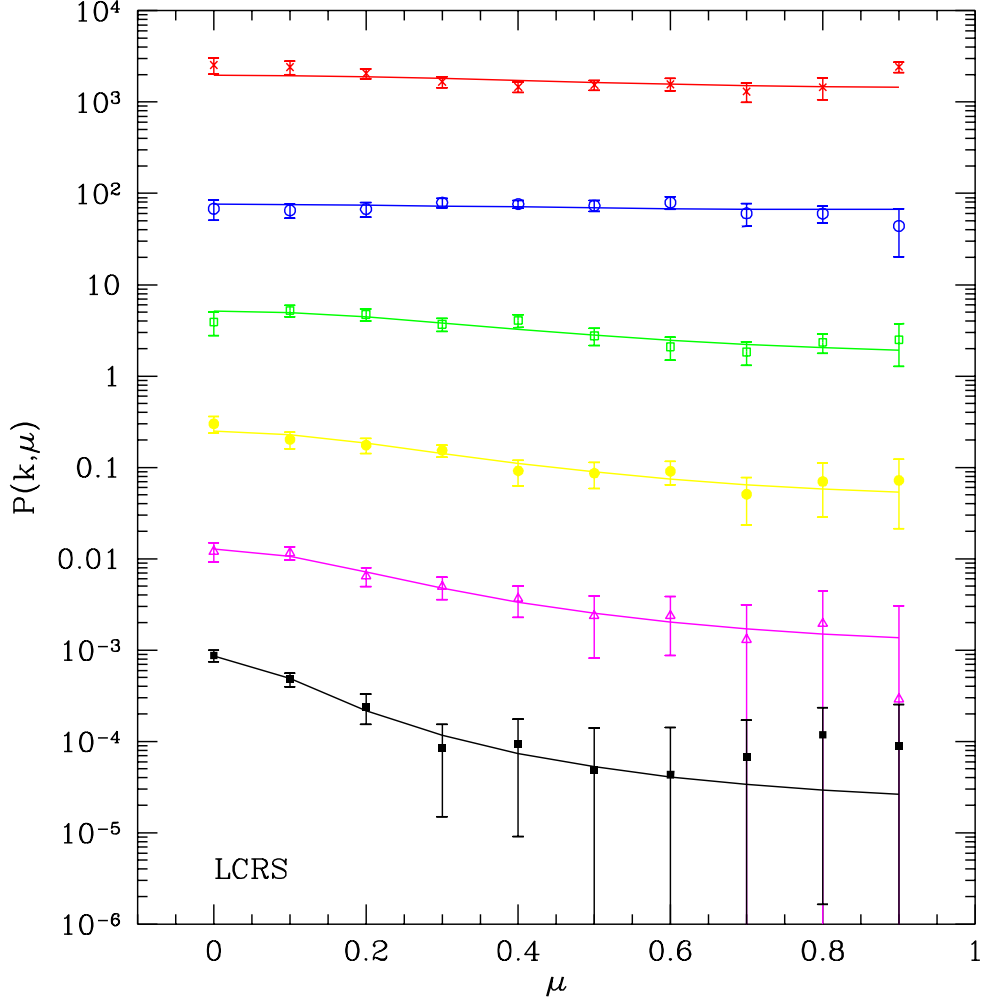


Fig. 2.— The redshift power spectrum  $P^S(k, \mu)$  of the Las Campanas Redshift Survey. The solid lines are the best-fit curves for free parameters  $\sigma_v$  and  $P^R(k)$ , assuming the Lorentz form for the damping function. Different colors correspond to different values of  $k$ . From top to bottom,  $k = 0.25$  to  $2.5 \, h\text{Mpc}^{-1}$  at  $\Delta \lg k = 0.2$ .

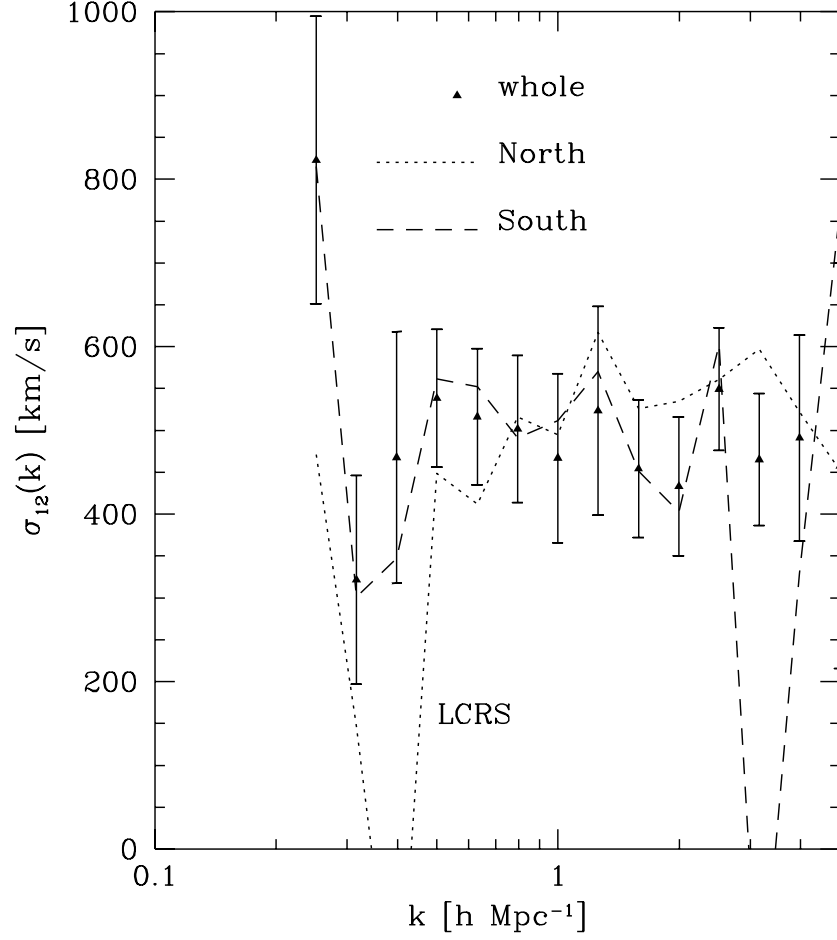


Fig. 3.— The pairwise velocity dispersion determined from the redshift power spectrum for the Las Campanas Redshift Survey. The whole sample, the south subsample, and the north subsample are represented by the triangles (with error bars), the dashed and the dotted lines (without error bars) respectively.

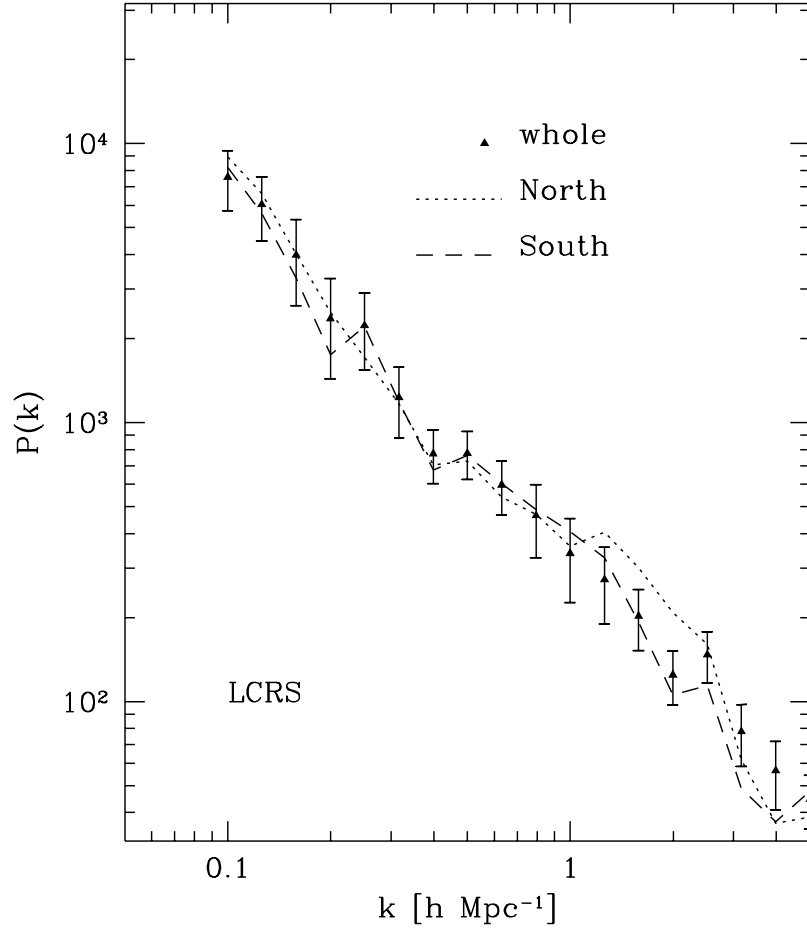


Fig. 4.— The real space power spectrum determined from the redshift power spectrum for the Las Campanas Redshift Survey. The whole sample, the south subsample, and the north subsample are represented by the triangles (with error bars), the dashed and the dotted lines (without error bars) respectively.

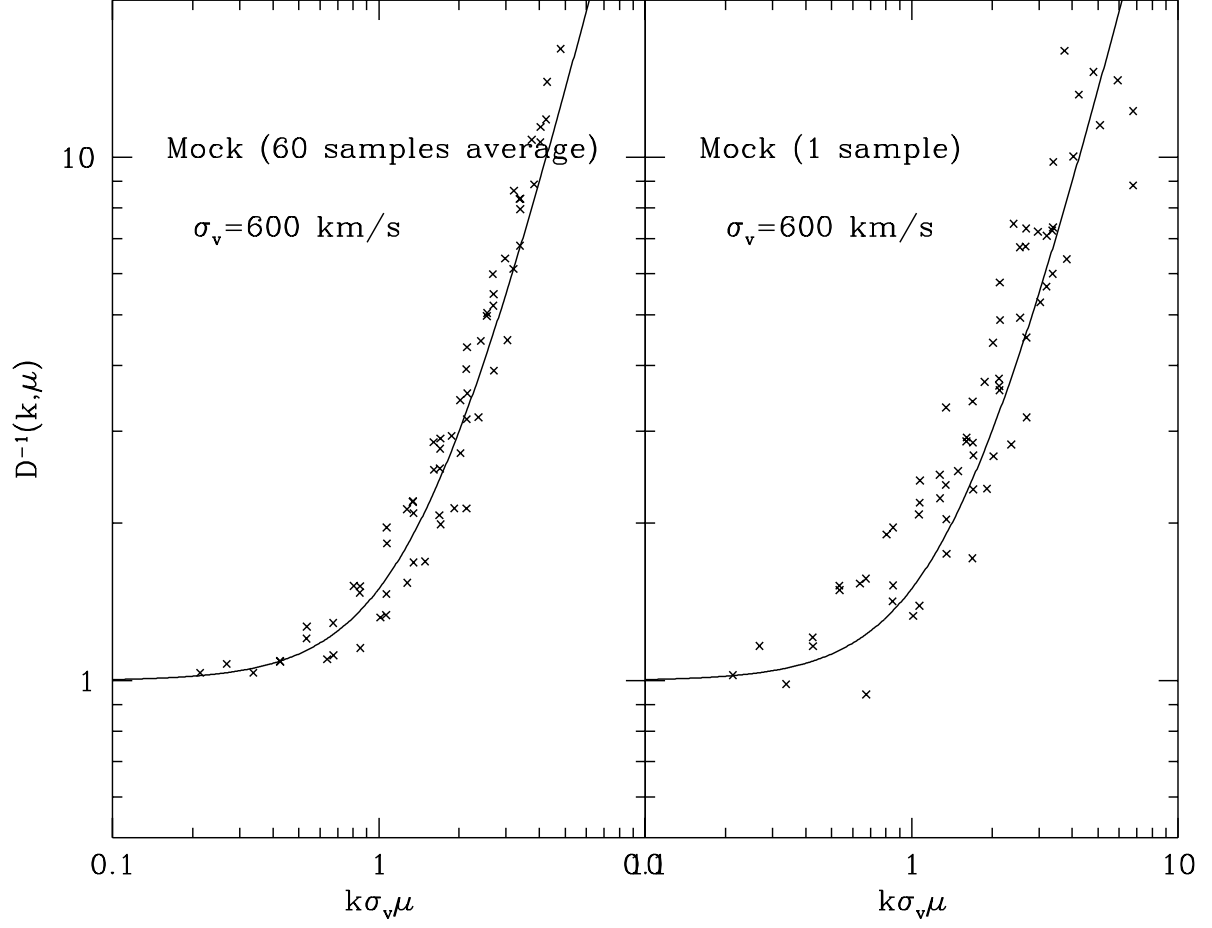


Fig. 5.— The inverse of the damping function  $D(k, \mu)$  of the cluster-weight biased mock samples with  $\Omega_0 = 0.2$ , plotted as a function of  $k\mu\sigma_v$ . In this plot, we have set  $\sigma_v = 600 \text{ km s}^{-1}$ .



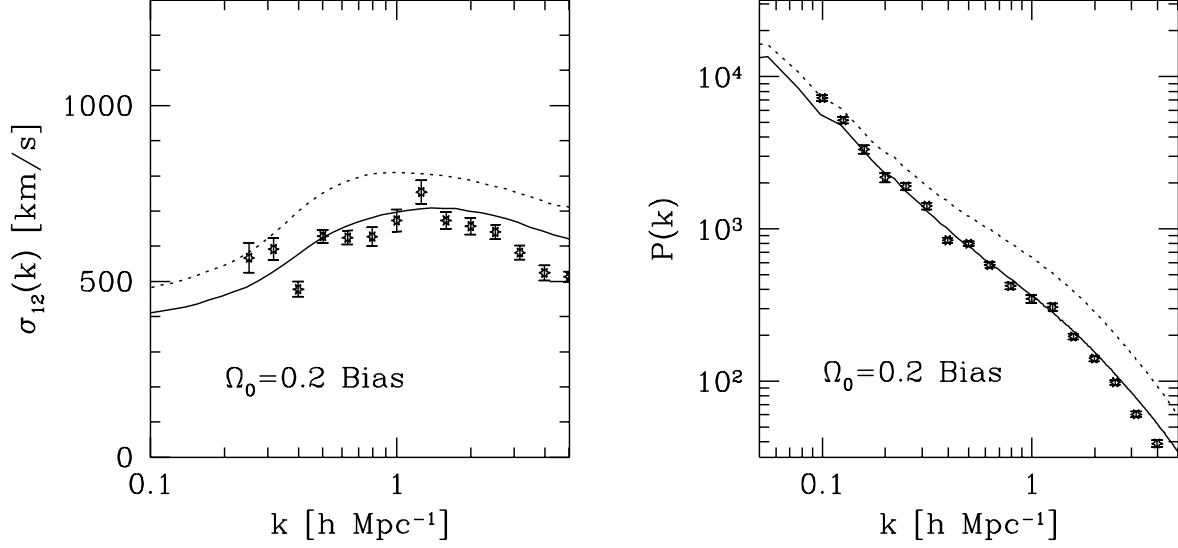


Fig. 6.— The pairwise velocity dispersion and real-space power spectrum determined for the 60 mock samples. The error bar is the expected  $1\sigma$  error of the mean value of the 60 samples. The solid lines are the pairwise velocity dispersion measured from the peculiar velocity (assuming  $k = 1/r$  for the plot) and the real-space power spectrum from the particle spatial coordinates. Similar to the solid lines, the dashed ones are measured from the full simulations but without the cluster-weighted bias.

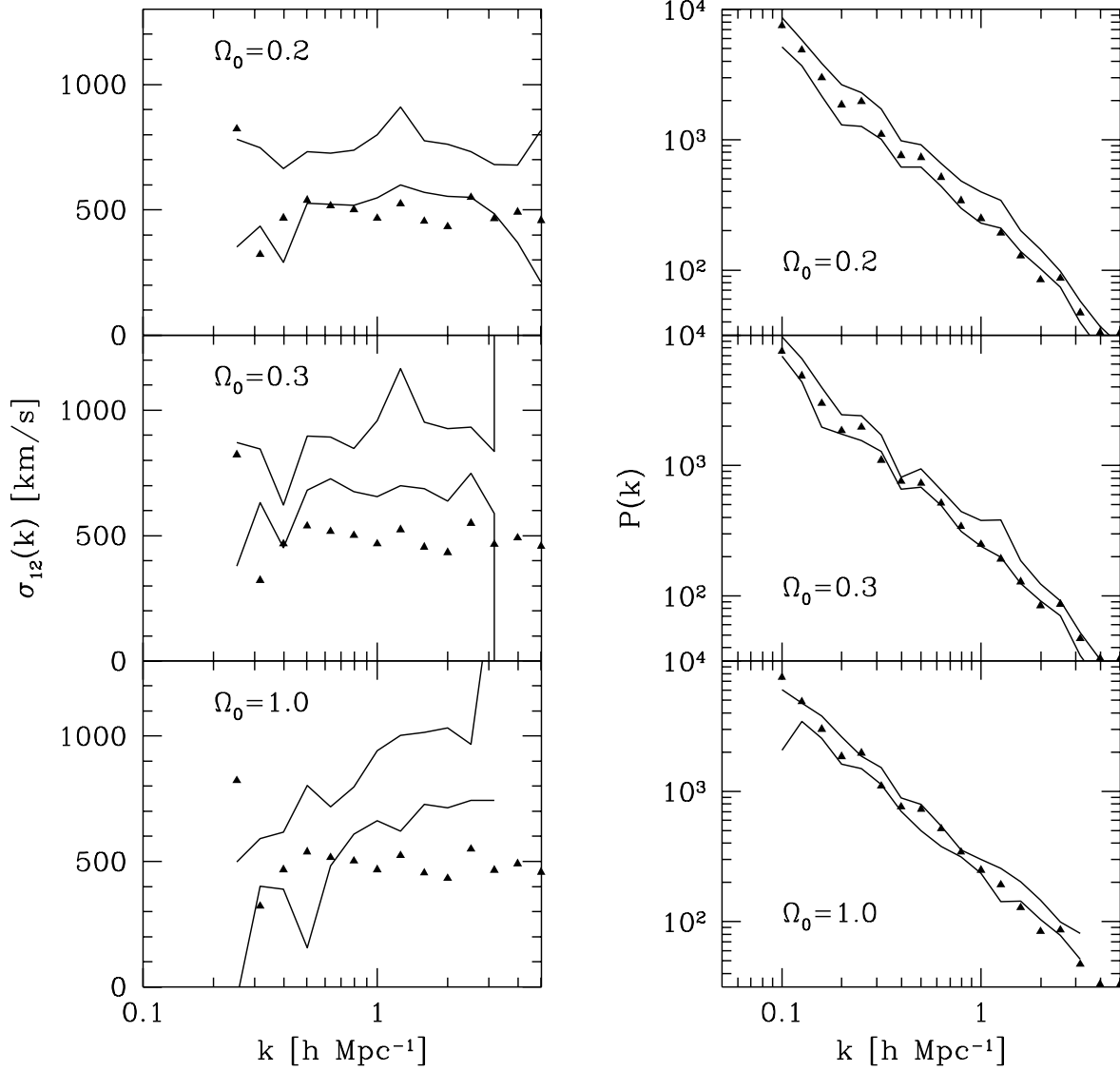


Fig. 7.— The pairwise velocity dispersion and real-space power spectrum determined for the Las Campanas Redshift Survey, compared to three CDM models with the cluster-weighted bias. The triangles are the results of the LCRS, and the lines are the  $1\sigma$  upper and lower limits of the CDM models.